

Behavior in Solution and Mixing Ratio-Dependent Binding Modes of Carcinogenic Benzo[*a*]pyrene-7,8-dione to Calf Thymus DNA

Biao Jin,^{*} Sung Wook Han,[†] and Dong Jin Lee[‡]

Key Laboratory of Natural Resources of Changbai Mountain & Functional Molecules of the Ministry of Education, Instrumental Analytical Center, Yanbian University, Yanji 133002, P.R. China. *E-mail: jb1979_0@126.com

[†]School of Herb Medicine Resource, Kyungwon University, Kumi, Gyeongbuk 730-852, Korea

[‡]Department of Chemical Engineering, Kyungil University, Gyeongbuk 712-701, Korea

Received March 28, 2014, Accepted June 23, 2014

The behavior of benzo[*a*]pyrene-7,8-dione (BPQ) in aqueous solution and its interaction with native DNA was investigated using conventional absorption and linear dichroism (LD) spectroscopy. The appearance of a broad absorption maximum at long wavelengths and its proportional relationship to solvent polarizability suggested that BPQ adopts a aggregated state for all solutions examined. Disappearance of this absorption band at higher temperatures in aqueous solution also supported BPQ aggregation. When associated with DNA absorption spectral properties were essentially the same as that in aqueous solution. However, two isosbestic wavelengths were found in the concentration-dependent absorption spectrum of the BPQ-DNA complex, suggesting the presence of at least two or more DNA-bound BPQ species. Both species produced LD^r spectra whose magnitude in BPQ absorption region is larger or comparable to that in the DNA absorption region, suggesting that the molecular BPQ plane is near perpendicular relative to the local DNA helical axis. Therefore, BPQ molecules are aligned along the DNA stem in both DNA-aggregated BPQ species.

Key Words : DNA, Benzo[*a*]pyrene-7,8-dione, Binding mode, Stacking, Linear dichroism

Introduction

Polycyclic aromatic hydrocarbons (PAHs) are ubiquitous environmental pollutants that are thought to cause cancer. The chemical carcinogenesis of PAHs, including benzo[*a*]pyrene (BP), a representative compound of the PAH family, has been a subject of intense study. In living cells, BP is metabolized to a variety of carcinogenic derivatives, including (±)-*anti*-7β,8α-dihydroxy-9α,10α-epoxy-7,8,9,10-tetrahydrobenzo[*a*]pyrene (*anti*-BPDE),¹⁻⁴ a radical cation that arises from one-electron oxidation at the C6 position on BP,⁵⁻⁷ and benzo[*a*]pyrene-7,8-dione (referred to as BPQ, Figure 1).⁸⁻¹⁰ *Anti*-BPDE damages DNA by forming predominantly N²-deoxyguanosine adducts within DNA,¹⁻⁴ while the radical cation forms depurinating adducts at the N7 position of adenine and the N7 and C8 positions of guanine.^{5,7} 7,8-Dihydroxy BP, which is the active form of BPQ, can be produced by the action of dihydrodiol dehydrogenase.⁹⁻¹¹ A variety of pathways resulting in damage to DNA by 7,8-dihydroxy BP, including oxidative DNA damage and the formation of DNA adducts, are known.¹¹⁻¹⁹ Reaction of BPQ with DNA yields multiple adducts; the predominant species are believed to consist of BPQ-deoxyguanosin adducts.^{18,19}

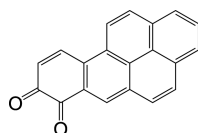


Figure 1. Chemical structure of BPQ.

In order to elucidate the mechanism of BPQ-DNA adduct formation, the elucidation of structural information regarding the physical complex that forms between BPQ and DNA may be essential. In the case of *anti*-BPDE, the structure of the *anti*-BPDE-DNA complex has been investigated extensively by various methods, including linear dichroism (LD) and fluorescence techniques.²⁰ Upon mixing with DNA, *anti*-BPDE rapidly intercalates between DNA base-pairs, at which point it either hydrolyzes to non-toxic benzo[*a*]pyrene-7,8,9,10-tetraol or forms adducts with DNA, mainly with guanine.²¹ Similarly, it is natural to assume that BPQ must associate with DNA prior to chemical reaction with the components of DNA. However, to our knowledge, there is no information available on the structure of the physical complex formed between BPQ and DNA. Therefore, in this work, we investigated the structure of the BPQ-DNA complex and the behavior of BPQ under various solution conditions mainly by means of normal absorption and LD spectroscopic analysis. We report the existence of at least two distinctive structures in the BPQ-DNA complex that are dependent on the [BPQ]/[DNA] ratio employed.

Experimental

Chemicals. All chemicals were purchased from Sigma-Aldrich except for BPQ, which was purchased as a powder from MRIGlobal. BPQ was dissolved in THF prior to use. DNA were dissolved in a 5 mM cacodylate buffer (pH 7.0) containing 1 mM ethylenediaminetetraacetic acid (EDTA) and 100 mM NaCl by gentle shaking at 4 °C, followed by

several times dialysis in a 5 mM cacodylate buffer (pH 7.0). The latter buffer was used for the BPQ-DNA binding study. The concentrations of DNA and BPQ were determined spectrophotometrically using the extinction coefficients of $\epsilon_{258\text{ nm}} = 6,700\text{ cm}^{-1}\text{M}^{-1}$ and $\epsilon_{347\text{ nm}} = 39,893\text{ cm}^{-1}\text{M}^{-1}$ (as provided by MRIGlobal) in buffer for DNA and in THF for BPQ, respectively. Aliquots of BPQ in THF were added to a DNA solution to obtain the desired mixing ratio, R , which is defined as the ratio $[\text{BPQ}]/[\text{DNA base}]$, and volume corrections were made. Typically less than 10 μL of BPQ in THF was added to 2 mL of the desired solutions for absorption measurements in the various solutions.

Measurements. LD is one of the most powerful spectroscopic techniques for determining the orientation of DNA-bound drugs relative to the DNA helical axis.^{20–22} LD is defined by $A_{\parallel}-A_{\perp}$, where A_{\parallel} and A_{\perp} are the absorbances measured with the polarization vector of the incident light beam oriented parallel and perpendicular, respectively, relative to the flow direction. Reduced LD (LD^r), a dimensionless quantity, is obtained by division of LD by isotropic absorption. LD^r is related to the angle, α , that specifies the orientation of the transition moment of drug relative to the local DNA helical axis (optical factor O) and the orientation ability of the drug-DNA complex in the flow (orientation factor S).

$$\text{LD}^r(\lambda) = \frac{\text{LD}(\lambda)}{A_{\text{iso}}(\lambda)} = S \times O(\lambda) = 1.5S \sum F_i (3\cos^2\alpha_i - 1) \quad (1)$$

Here, $F_i = \epsilon(\lambda)_i / \sum \epsilon(\lambda)_i$ denotes the contribution of i th component to the absorption at the particular wavelength λ . In general, a larger or comparable LD^r magnitude in the drug's absorption region compared to the DNA absorption region suggests that the ligand molecular plane is parallel to DNA base planes, or perpendicular to the local DNA helical axis. However, a positive signal in the drug's absorption region has been observed for the drug bound at the minor grooves.

Absorption spectra were recorded on either Jasco V 550 or Cary 500 instruments. LD spectra were measured on either J-715 or J-810 spectropolarimeters (Jasco, Tokyo, Japan) equipped with an inner rotating flow cell. All measurements were performed at room temperature except otherwise specified. Measured LD is divided by isotropic absorption to give the reduced.

Results

Absorption Spectra of BPQ in Various Solutions. The absorption spectra of BPQ in various solutions are shown in Figure 2(a). In aqueous solution, the spectrum consisted of two broad bands centered at $\sim 324\text{ nm}$ and $\sim 586\text{ nm}$. As the polarity of the solution decreased, the maximum at the longer wavelength shifted to a shorter wavelength. Vibronic structures started to appear for both short- and long-wavelength absorption bands as the polarity decreased. For instance, the vibronic structures in the pyrene absorption region at 329 nm and 344 nm were apparent in hexane. The

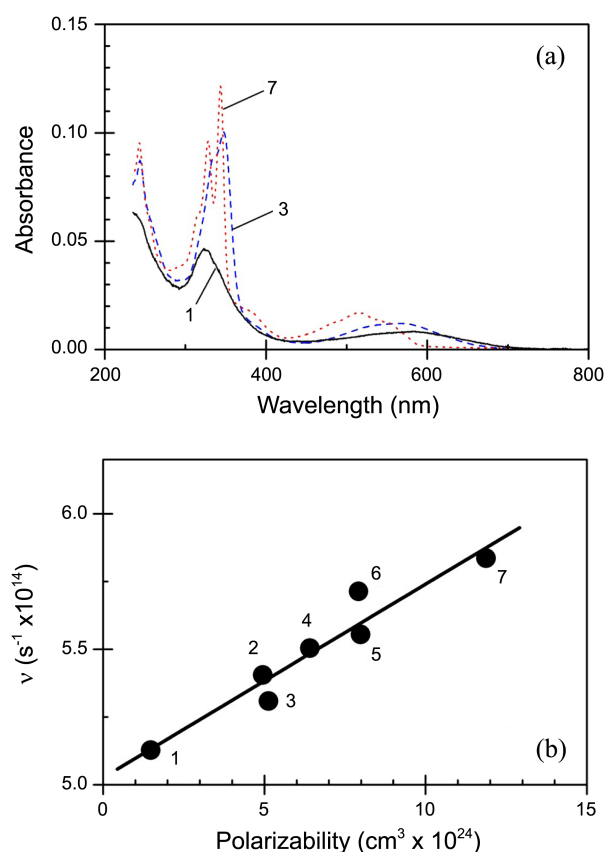


Figure 2. (a) Representative absorption spectrum of BPQ in various solutions. $[\text{BPQ}] = 2.4\text{ }\mu\text{M}$. Solid curve (number 1): in water; dashed curve (number 3): in ethanol; dotted curve (number 7): in hexane. Absorption spectrum in water is enlarged twice for easy of comparison. (b) The maximum frequency at the lowest energy with respect to the solution polarizability. From number 1 through 7, the solution is water, acetonitrile, ethanol, acetone, THF, DMSO and hexane.

broad absorption band at the long wavelength shifted to a shorter wavelength of 420–580 nm in hexane. In ethanol, these two absorption bands were observed at $\sim 347\text{ nm}$ and 567 nm with a shoulder at $\sim 334\text{ nm}$. A fair correlation was found when the maximum frequencies of the absorption bands at lower energies (long wavelengths) were plotted with respect to solvent polarizability (Figure 2(b)), suggesting that the absorption band at the long wavelength is related to the stacking or self-association of BPQ.

The absorption spectra measured at a variety of pHs are depicted in Figure 3. As shown, the shape of the BPQ absorption spectrum in aqueous solution was strongly dependent on the solution pH. In the pH range of 2.0–10.0 (using the 5 mM cacodylate buffer), the absorption spectrum was characterized by two broad bands with their maxima at $\sim 324\text{ nm}$ and $\sim 586\text{ nm}$, as mentioned above. However, in the pH range 10.0–12.0, a drastic change in absorption spectrum shape was observed in both the pyrene absorption region and the long-wavelength region. The broad band at the longer wavelength started to disappear, with the appearance of a vibronic structure at 300–360 nm as the pH increased. At pH 12.0, the absorption spectrum of BPQ was characterized by

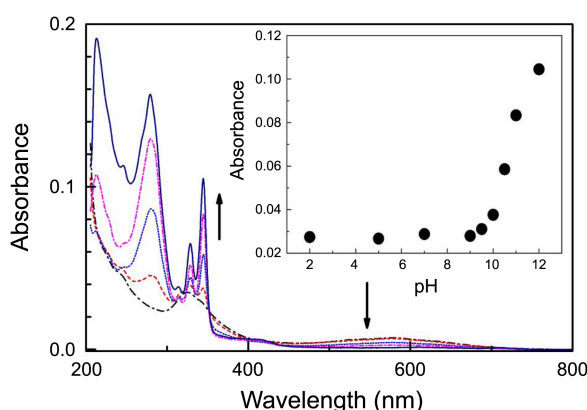


Figure 3. Absorption spectrum of BPQ (5.0 μ M) at the various pHs in 5 mM cacodylate buffer. To the arrow direction, pH is 9.0, 10.0, 10.5, 11.0, 12.0. Note that the vibronic structures are apparent at high pH and that the absorption spectra are identical at the pH below 9.0. Insertion: Change in absorbance of BPQ at 345 nm with pH.

sharp vibronic bands at 314 nm, 329 nm, and 345 nm, similar to those observed for monomeric pyrene. At this high pH, the broad band at \sim 586 nm completely disappeared, suggesting that the band at the longer wavelength is related to the deprotonation of the carbonyl moiety of BPQ. The change in absorbance at 345 nm with respect to pH change is

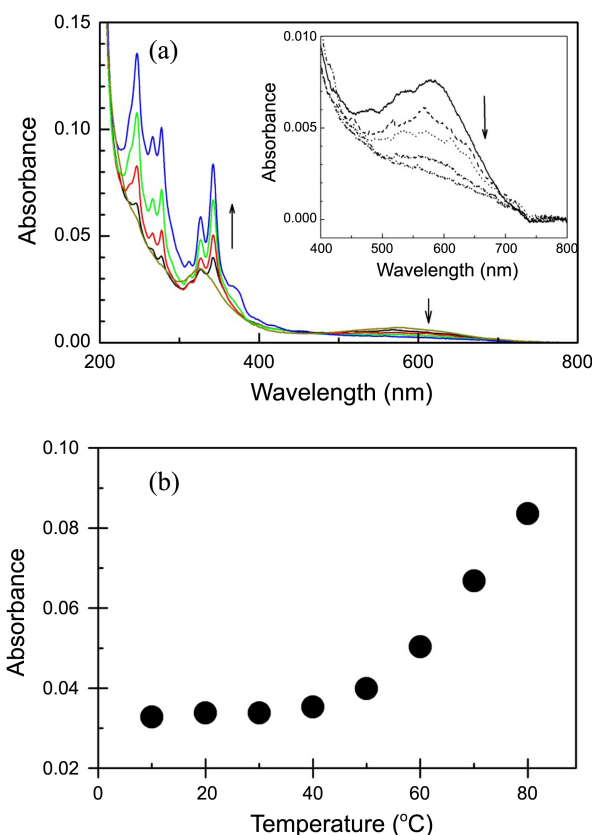


Figure 4. (a) Absorption spectrum of BPQ at the various temperatures. To the arrow direction: temperature is 20, 50, 60, 70 and 80 $^{\circ}$ C. (b) Absorbance of BPQ at 345 nm with respect to the temperature.

also shown in Figure 3 as an insert. As can be clearly seen, a protonation–deprotonation equilibrium occurred between pH 10.0 and 12.0. Disappearance of the broad band at the longer wavelength and the appearance of vibronic structures in the pyrene suggested that BPQ is in its monomeric form at high pH.

The shape of the BPQ absorption spectrum was also found to be dependent on temperature. The temperature-dependent absorption spectrum of BPQ at pH 7.0 is depicted in Figure 4(a).

An enlarged absorption spectrum at long wavelength is inserted. Figure 4(b) shows the changes in absorbance at 342 nm with respect to temperature. At a temperature below 40 $^{\circ}$ C, the appearance of the absorption spectrum was similar to that at low pH, *i.e.*, characterized by two broad bands at \sim 324 nm and \sim 585 nm. At 50 $^{\circ}$ C, the vibronic structure in the short absorption band started to appear, and absorbance at the longer wavelength was decreased. At a temperature of 70 $^{\circ}$ C, vibronic bands at 312 nm, 326 nm, and 342 nm were apparent, while the broad band at the longer wavelength completely disappeared. The shape of the absorption spectrum was similar to that obtained at a high pH. This observation suggested that BPQ forms a complex with other BPQ molecules at a temperature below 60 $^{\circ}$ C. When the temperature was further increased, a new shoulder appeared at ca. 370 nm. In the case of pyrene, a symmetry-forbidden absorption band in this region is known.²⁶

Absorption and LD Spectra of the BPQ–DNA Complex.

The absorption spectra of the BPQ–DNA complex were recorded at various BPQ concentrations in the presence of a fixed concentration of DNA. The corresponding DNA spectrum was subtracted from those of the mixtures, and then resulting spectra were normalized to the highest concentration of BPQ for easy comparison (Figure 5(a)).

The absorption spectra of BPQ complexed with DNA at various *R* ratios showed four clear isosbestic wavelengths at 337 nm, 401 nm, 458 nm, and 586 nm, suggesting the presence of two DNA-bound BPQ species. At a low *R* ratio, two broad absorption bands at 361 nm and 624 nm were apparent (referred to as Species I). Compared to its spectrum in the absence of DNA, this species exhibited a 38 nm red-shift at both short and long wavelengths, and the absorbance at the shorter wavelength increased almost two-fold (Figure 5(b)). As the *R* ratio was increased, a second species was produced with two absorption bands at 327 nm and 575 nm (referred to as Species II). The shape of the absorption spectrum of Species II resembled but was not identical to that of the DNA-free BPQ in aqueous solution (Figure 5(b)). The shifts in absorption maxima compared to BPQ in the aqueous solution were determined as 4 nm and 10 nm, respectively, at the short and long wavelengths. The extent of the increase in absorbance, when compared to BPQ in the absence of DNA, was less than that of Species I. Species II, which dominates at a high *R* ratio, is likely not assigned to a BPQ molecule that is not associated with DNA, since this species exhibited not only changes in its absorption spectrum, but also displayed a strong LD signal. The equilibrium

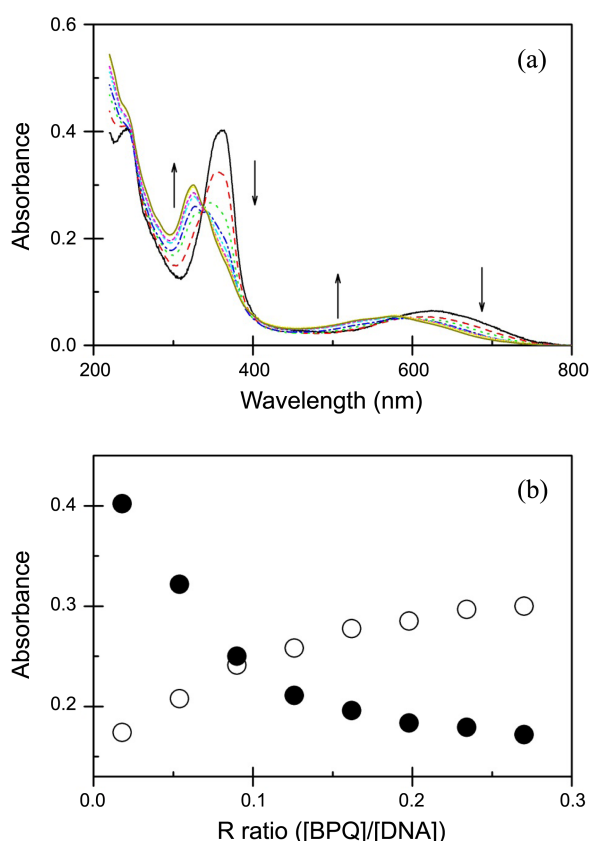


Figure 5. Absorption spectrum of BPQ in the presence of DNA (panel (a)). [DNA] = 100 μ M. To the arrow direction, [BPQ] = 1.8, 5.6, 8.8, 12.2, 15.6, 18.9, 22.1 and 25.3 μ M. Absorption spectrum was obtained by subtracting DNA absorption from the complex and normalized to the highest concentration of BPQ. Changes in the absorbance at 325 nm (open circles) and 360 nm (closed circles) are depicted in panel (b) with respect to the [BPQ]/[DNA base] ratio.

of these two species at a low and high R ratio was accompanied by two isosbestic points at 337 nm and 586 nm, suggesting that there are no other absorbing BPQ species in the system, unless the absorption spectrum of the third species is coincidentally identical with any of the first two species, which is highly improbable. It is notable that, although Species II was dominant at a high R ratio, it started to appear even at a very low R ratio (Figure 5(a), insert). Both species appeared to be saturated at a mixing ratio above 0.25.

LD and LD^r spectra of the BPQ–DNA complex at various R ratios are depicted in Figures 6(a) and (b), respectively.

For this measurement, the concentration of BPQ was fixed and that of DNA was varied to obtain the desired mixing ratios. At a glance, a strong negative band at 361 nm at a low mixing ratio ($R = 0.02$) was apparent. As the mixing ratio was increased, the relative intensity of this band decreased with the appearance of a new LD band at a shorter wavelength. The negative LD features of both species immediately exclude the possibility that the BPQ molecule binds in the minor groove of DNA. If the BPQ were to bind in the minor groove, the angle of the $\pi^* \leftarrow \pi$ electric transition of the

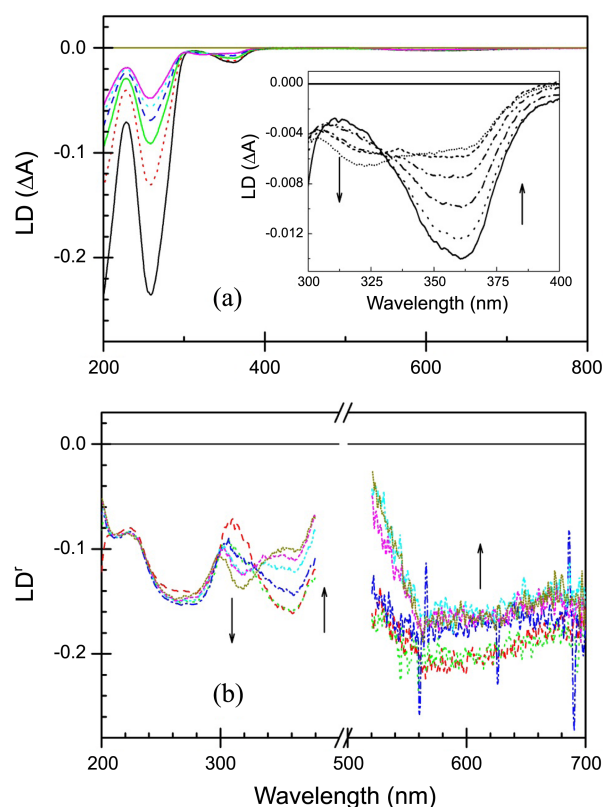


Figure 6. (a) LD spectrum of the BPQ–DNA complex at the various [BPQ]/[DNA base] ratios. [BPQ] = 5.0 μ M. The mixing ratios are 0.02, 0.04, 0.06, 0.08, 0.10 and 0.12 to the arrow direction. (b) LD^r spectrum of the BPQ–DNA complex obtained by dividing the LD by isotropic absorption spectrum. The condition and the concentrations are the same as in the panel (a).

aromatic moiety should be 45° relative to the DNA helical axis. Hence, a positive LD is expected. Although not clearly visible, a negative LD band at the longer wavelength was apparent. The magnitude of the LD^r spectrum of Species I for both absorption bands was larger than that of the DNA at 260 nm (Figure 6(b)). A larger LD^r magnitude in the drug's absorption region compared to that in the DNA absorption region is typical for drugs intercalating between DNA base-pairs;²⁴ therefore, the plane of BPQ is parallel to the DNA base-pairs. However, in the case of Species II, a smaller magnitude in the drug's absorption region appeared compared to that in the DNA absorption region, suggesting that the $\pi^* \leftarrow \pi$ electric transition of the aromatic moiety of Species II is strongly tilted with respect to the DNA helical axis. A significant decrease in the LD^r magnitude between 500 nm and 570 nm, where Species II absorption is dominant, supported the possibility of a tilt of the BPQ plane relative to the DNA helical axis. Essentially, the same mixing ratio–dependent spectral properties were found for the DNA–BPQ complex in which the concentration of DNA is fixed at 100 μ M and that of the BPQ varies from 2.0 μ M to 10.0 μ M.

Discussion

Behavior of BPQ in Solutions. The shape of BPQ's

absorption spectrum in various solutions is characterized by a weak broad band at a longer wavelength, a second absorption band in the 300–350 nm region, and another below 300 nm. Considering that the transition from the ground state to S1 state is forbidden, the absorption band in the 300–350 nm wavelength region represents the transition from the ground state to the S2 electronic state, and that in the higher-energy region represents the transition to the S3 state. The maximum of the broad band observed in the longer-wavelength region was proportional to the medium polarizability, reflecting the occurrence of aggregation.^{23,25} As the polarizability increased, the vibronic structure of the transition to the S2 state became clearer. The shape of the absorption spectrum is affected by both pH and temperature. At a high temperature (Figure 4), the broad band located at the longer wavelength disappeared, and the vibronic structure for the S2 transition became clearer; in contrast, a featureless absorption band was observed in the long-wavelength and 300–350 nm region at a low temperature, supporting the aggregation/stacking of BPQ at a low temperature. Change in the absorption spectrum was also associated with pH of the medium (Figure 3). At a high pH, at which the BPQ molecule is probably deprotonated, the broad band at the longer wavelength disappeared, and the vibronic structure at 300–350 nm region became clear, suggesting that BPQ exists as the monomeric form. As one of the carbonyl groups of BPQ is protonated, the shape of the absorption spectrum resembles that observed at a low temperature, suggesting that the protonated BPQ species is the one involved in the formation of aggregation/stacking. When one of the carbonyl group is protonated, BPQ can form a dimer and/or oligomer with other BPQs via intermolecular hydrogen-bond formation. Therefore, it is conceivable that, in addition to the simple π - π interactions in the aggregated/stacked BPQ, the formation of intermolecular hydrogen bonds is also possible.

Stacking of BPQ Along the DNA Stem. When associated with DNA in aqueous solution at pH 7.0, BPQ clearly produced two absorbing species dependent on the R ratio. Four isosbestic wavelengths were found for the relative concentration-dependent absorption spectrum of the BPQ–DNA complex, suggesting the presence of at least two or more bound BPQ species. The broad absorption band at longer wavelengths observed for both Species I and II suggests that BPQ is in the aggregated/stacked form, even when associated with DNA. As the R ratio increased, this absorption band shifted to the shorter wavelength, suggesting that Species I is in a less polar environment compared to Species II (having the higher R ratio form). No evidence for the presence of monomeric BPQ bound to DNA was observed. When the R ratio reached ca. 0.25, Species II was found to be dominant.

Upon binding to DNA, BPQ produced a negative LD spectrum both in the 300–350 nm and long-wavelength regions, suggesting that the molecular plane of the BPQ molecule is near parallel with respect to the DNA base plane. Considering that the in-plane electric transition moment of the groove-binding molecules tilt from the local DNA helical

axis at about 45°, which results in a positive LD signal in the absorption region of the bound DNA bound molecule, the observed negative LD removes the possibility of a groove-binding mode for BPQ. In the LD^r spectra, the magnitude of BPQ in the 360–380 nm absorption region at a high R ratio and 320–330 nm absorption region at low R ratios was comparable with that of DNA. At all R ratios, the LD^r magnitude at long wavelength was larger or comparable with that in the DNA absorption region. This LD^r observation for the BPQ–DNA complex indicated that the molecular plane of BPQ is near parallel relative to the DNA base plane or perpendicular to the local DNA helical axis.^{20–22} A parallel binding geometry between DNA base planes and the molecular plane of the DNA-bound drug usually indicates an intercalative binding mode for the drug. However, given that BPQ forms either an aggregate or stacks upon binding to DNA, intercalation of BPQ between DNA base-pairs is not likely to occur since the separation of DNA base-pairs—a requirement for the intercalation of aromatic compounds—to allow intercalation of two or more stacked aromatic compound is impossible. In the aggregate, BPQ is aligned in a way that its molecular plane is near perpendicular to the local DNA helical axis. In other words, BPQ stacks along the DNA stem. As judged from its pH-dependent absorption spectrum, protonated BPQ might be connected by hydrogen bonds in aqueous solution. The appearance of a similar absorption spectrum suggested the possibility of a similar hydrogen-bond formation mechanism of protonated BPQ upon association with DNA. In the BPQ stack along the DNA stem, π - π interaction between aromatic rings might also take on an important role. Although the exact nature of the two stacked BPQ species cannot be specified at this stage, the complex formed at lower R ratio is in a less polar environment than that at high R ratios.

Conclusion

In this study, the behavior of BPQ in aqueous solution and its interaction with native polynucleotides was investigated using conventional absorption and LD spectroscopy. Under physiological conditions, one of the carbonyl moieties of BPQ is protonated; when protonated, BPQ molecules can associate through hydrogen bonds to form a dimer. The dimers are stacked along the DNA stem through π - π interactions. Stacked BPQ can be categorized into two species when associated with DNA. The exact nature of stacked BPQ is unclear at this stage, and requires further investigation.

Acknowledgments. This study was supported by National Natural Science Foundation of China (grant no. 21265022).

References

1. Jennette, K. W.; Jeffrey, A. M.; Blobstein, S. H.; Beland, F. A.; Harvey, R. G.; Weinstein, I. B. *Biochemistry* **1977**, *16*, 932.
2. Conney, A. H. *Cancer Res.* **1982**, *42*, 4875.

3. Shimada, T.; Gillam, E. M.; Oda, Y.; Tsumura, F.; Sutter, T. R.; Guengerich, F. P.; Inoue, K. *Chem. Res. Toxicol.* **1999**, *12*, 623.
 4. Shimada, T.; Oda, Y.; Gillam, E. M.; Guengerich, F. P.; Inoue, K. *Drug Metab. Dispos.* **2001**, *29*, 1176.
 5. Devanesan, P. D.; RamaKrishna, N. V. S.; Todorovic, R.; Rogan, E. G.; Cavalieri, E. L.; Jeong, H.; Jankowiak, R.; Small, G. J. *Chem. Res. Toxicol.* **1992**, *5*, 302.
 6. Cavalieri, E. L.; Rogan, E. G. *Xenobiotica* **1995**, *25*, 677.
 7. Chen, L.; Devanesan, P. D.; Higginbotham, S.; Ariese, F.; Jankowiak, R.; Small, G. J.; Rogan, E. G.; Cavalieri, E. L. *Chem. Res. Toxicol.* **1996**, *9*, 897.
 8. Palackal, N. T.; Burczynski, M. E.; Harvey, R. G.; Penning, T. M. *Biochemistry* **2001**, *40*, 10901.
 9. Palackal, N. T.; Lee, S. H.; Harvey, R. G.; Blair, I. A.; Penning, T. M. *J. Biol. Chem.* **2002**, *277*, 24799.
 10. Penning, T. M.; Burczynski, M. E.; Hung, C.-F.; McCoull, K. D.; Palackal, N. T.; Tsuruda, L. S. *Chem. Res. Toxicol.* **1999**, *12*, 1.
 11. Penning, T. M.; Ohnishi, P. S. T.; Ohnishi, T.; Harvey, R. G. *Chem. Res. Toxicol.* **1996**, *9*, 84.
 12. Kasai, H.; Crain, P. F.; Kuchino, Y.; Nishimura, S.; Ootsuyama, A.; Tanooka, H. *Carcinogenesis* **1986**, *7*, 1849.
 13. Frenkel, K. *Pharmacol. Ther.* **1992**, *53*, 127.
 14. Chaudhary, A. K.; Nokubo, M.; Reddy, G. R.; Yeola, S. N.; Morrow, J. D.; Blair, I. A.; Marnett, L. J. *Science* **1994**, *265*, 1580.
 15. Benamira, M.; Johnson, K.; Chaudhary, A.; Bruner, K.; Tibbets, C.; Marnett, L. J. *Carcinogenesis* **1995**, *16*, 93.
 16. DeMarini, D. M.; Brockman, H. E.; deSerres, F. J.; Evans, H. H.; Stankowski, L. F.; Hsie, A. W. *Mutat. Res.* **1989**, *220*, 11.
 17. Emerit, I.; Keck, M.; Levy, A.; Feingold, J.; Michelson, A. M. *Mutat. Res.* **1982**, *103*, 165.
 18. Balu, N.; Padgett, W. T.; Lambert, G. R.; Swank, A. E.; Richard, A. M.; Nesnow, S. *Res. Toxicol.* **2004**, *17*, 827.
 19. Balu, N.; Padgett, W. T.; Nelson, G. B.; Lambert, G. R.; Ross, J. A.; Nesnow, S. *Anal. Biochem.* **2006**, *355*, 213.
 20. Nordén, B.; Kubista, M.; Kurucsev, T. *Q. Rev. Biophys.* **1992**, *25*, 51.
 21. Nordén, B.; Kurucsev, T. *J. Mol. Recognit.* **1994**, *7*, 141.
 22. Nordén, B.; Rodger, A.; Dafforn, T. *Linear Dichroism and Circular Dichroism*; RSC Pub.: U.K. 2010.
 23. Silvina Fioressi, E.; Binning, R. C., Jr.; Bacao, Daniel E. *Chem Phys Lett.* **2008**, *454*, 269.
 24. Tuite, E.; Nordén, B. *Bioorg. Med. Chem.* **1995**, *3*, 701.
 25. Nath, S.; Pal, H.; Sapre, A. V. *Chem. Phys. Lett.* **2000**, *327*, 143.
 26. Khakhel, O. A. *J. Appl. Spectrosc.* **2001**, *68*, 280.
-